Article:

Mullaney, J.R., Alexander, D.M., Aird, J. et al. (15 more authors) (2015) ALMA and Herschel reveal that AGN and main-sequence galaxies have different star formation rate distributions. (Submitted)

ALMA and *Herschel* reveal that AGN and main-sequence galaxies have different star formation rate distributions

J. R. Mullaney[1]⋆, D. M. Alexander[2], J. Aird[3], E. Bernhard[1], E. Daddi[4], A. Del Moro[2], M. Dickinson[5], D. Elbaz[4], C. M. Harrison[2], S. Juneau[4], D. Liu[4], M. Pannella[6], D. Rosario[7], P. Santini[8], M. Sargent[9], C. Schreiber[4], J. Simpson[2], F. Stanley[2]

[1]*Department of Physics and Astronomy, The University of Sheffield, Hounsfield Road, Sheffield, S3 7RH, UK*
[2]*Centre of Extragalactic Astronomy, Department of Physics, Durham University, South Road, Durham, DH1 3LE, UK*
[3]*Institute of Astronomy, University of Cambridge, Madingley Road, Cambridge CB3 0HA, UK*
[4]*Laboratoire AIM, CEA/DSM-CNRS-Université Paris Diderot, Irfu/Service dAstrophysique, CEA-Saclay, Orme des Merisiers, 91191 Gif-sur-Yvette, France*
[5]*National Optical Astronomy Observatories, 950 N Cherry Avenue, Tucson, AZ 85719, USA*
[6]*Universitäts-Sternwarte München, Scheinerstr. 1, D-81679 München*
[7]*Max-Planck-Institut fr Extraterrestrische Physik (MPE), Postfach 1312, 85741, Garching, Germany*
[8]*INAF-Osservatorio Astronomico di Roma, via di Frascati 33, I-00040 Monte Porzio Catone, Roma, Italy*
[9]*Astronomy Centre, Department of Physics and Astronomy, University of Sussex, Brighton, BN1 9QH, UK*

ABSTRACT

Using deep *Herschel* and ALMA observations, we investigate the star formation rate (SFR) distributions of X-ray AGN host galaxies at $0.5 < z < 1.5$ and $1.5 < z < 4$, comparing them to that of normal, star-forming (i.e., "main-sequence", or MS) galaxies. We find 34–55 per cent of AGNs have SFRs at least a factor of two below that of the average MS galaxy, compared to ≈ 15 per cent of all MS galaxies, suggesting significantly different SFR distributions. Indeed, when both are modelled as log-normal distributions, the mass and redshift-normalised SFR distributions of AGNs are roughly twice as broad, and peak ≈ 0.4 dex lower, than that of MS galaxies. However, like MS galaxies, the normalised SFR distribution of AGNs appears not to evolve with redshift. Despite AGNs and MS galaxies having different SFR distributions, the linear-mean SFR of AGNs derived from our distributions is remarkably consistent with that of MS galaxies, and thus with previous results derived from stacked *Herschel* data. This apparent contradiction is due to the linear-mean SFR being biased by bright outliers, and thus does not necessarily represent a true characterisation of the typical SFR of AGNs.

Key words: galaxies: active—galaxies: evolution—galaxies: statistics

1 INTRODUCTION

Today's most successful models of galaxy evolution predict that the energy released via accretion onto supermassive black holes (hereafter, BHs) has played an important role in dictating how today's galaxies have grown and evolved (e.g., Vogelsberger et al. 2014; Schaye et al. 2015). As such, understanding the connection between galaxy growth via star-formation and the growth of their resident BHs is one of the key challenges facing current extragalactic research (e.g. Alexander & Hickox 2012). There are now numerous lines of empirical evidence in support of time-averaged/integrated BH growth correlating with star-formation in their host galaxies; for example, (a) the tight proportionality between BH mass and galaxy bulge mass (e.g., Gebhardt et al. 2000); (b) the similar cos-

mic histories of the volume-averaged BH growth and star formation rates (hereafter, SFR; e.g., Silverman et al. 2008; Aird et al. 2015); and, more directly, (c) the correlation between average BH growth and SFR among the star-forming galaxy population (e.g., Mullaney et al. 2012b; Chen et al. 2013; Delvecchio et al. 2015; Rodighiero et al. 2015). However, it is still far from clear what physical processes (e.g., feedback processes/common fuel supply/common triggering mechanism) connect BH growth to star-formation to produce these average trends.

One of the primary means of making progress in this area has been to measure the SFRs and specific SFRs (i.e., SFR per unit stellar mass, or sSFR) of galaxies hosting growing BHs (witnessed as active galactic nuclei, or AGN) and search for correlations or differences (vs. the non-AGN population) that may signify a causal connection. The *Herschel Space Observatory* (hereafter, *Herschel*) has played a major role in progressing this science

⋆ E-mail: j.mullaney@sheffield.ac.uk
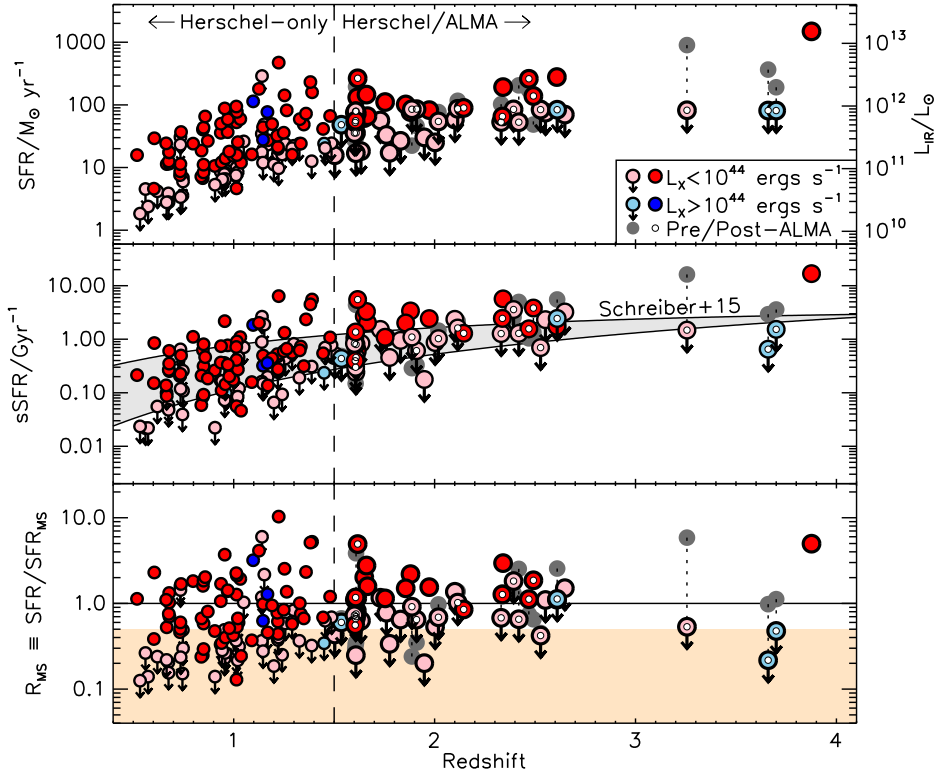
Figure 1. Host galaxy star-forming properties of our low-*z* (i.e., $0.5 < z < 1.5$; not observed by ALMA) and high-*z* (i.e., $z > 1.5$) samples of AGNs (samples separated by the vertical dashed line). In all plots, grey circles indicate pre-ALMA (specific) star formation rates ([s]SFRs) from *Herschel* which are connected to their ALMA-measured (s)SFRs by dotted lines. (s)SFRs from ALMA are indicated by small white circles. Red and blue circles represent AGNs with $L_X = 10^{42-44}$ ergs s^{-1} and $L_X > 10^{44}$ ergs s^{-1}, respectively, with lighter colours used for 3σ upper limits. *Top:* SFR vs. redshift. Despite our ALMA observations probing SFRs up to a factor of ≈ 10 lower than *Herschel*, only ≈ 29 per cent of our ALMA-targeted AGNs are detected. *Middle:* sSFR vs. redshift. In this panel, the shaded region represents the average sSFR of main-sequence (MS) galaxies (SFR$_{MS}$) as described by Eqn. 9 of S15 for the stellar mass range of our sample. *Bottom:* R_{MS} vs. redshift. By definition, the horizontal line represents the average R_{MS} of MS galaxies. Shading indicates where $R_{MS} < 0.5$. Between 34 and 55 per cent (dependent on upper limits) of AGNs in our combined (i.e., low-*z*+high-*z*) sample lie within this shaded region, compared to ≈ 15 per cent of MS galaxies.

by providing an obscuration-independent view of star-formation that is largely uncontaminated by emission from the AGN. However, with even the deepest *Herschel* surveys detecting $\lesssim 50$ per cent of the AGN population, most studies have resorted to averaging (often via stacking analysis, but see Stanley et al. 2015) to characterise the (s)SFRs of the AGN population. These studies have typically reported that the average SFRs of AGNs trace that of star-forming "main-sequence" (hereafter, MS) galaxies (e.g., Mullaney et al. 2012a; Santini et al. 2012; Harrison et al. 2012; Rosario et al. 2013; Stanley et al. 2015), i.e., the dominant population of star-forming galaxies whose SFRs are roughly proportional to their stellar mass (i.e., sSFR≈constant), with a constant of proportionality that increases with redshift (e.g., Noeske et al. 2007; Daddi et al. 2007). However, as averages can be biased by bright outliers, it is feasible that these findings are being driven upwards by a few bright sources (e.g., Fig. 14 of Rosario et al. 2015). Here, we test this by combining deep *Herschel* and ALMA observations to instead constrain the *distribution* of host galaxy SFRs of a sample of X-ray selected AGNs and comparing it to that of MS galaxies. We adopt $H_0 = 71$ km s^{-1} Mpc^{-1}, $\Omega_\Lambda = 0.73$, $\Omega_M = 0.27$ and a Chabrier initial mass function (IMF).

2 SAMPLE SELECTION

To allow us to investigate any redshift evolution of the AGN (s)SFR distribution, we use two samples of X-ray selected AGNs: a low-*z* sample spanning $0.5 \leqslant z < 1.5$ and a high-*z* sample spanning $1.5 \leqslant z < 4$ (although we note that the high-*z* is dominated by AGNs at $1.5 \leqslant z < 2.7$). The split at $z = 1.5$ is motivated by our ALMA target selection criteria: for this, we only consider AGNs with redshifts > 1.5 since (a) the majority of $z < 1.5$ AGNs are detected with *Herschel* in the deepest fields and thus already have obscuration-independent SFR measures and (b) the negative *k*-correction at sub-mm wavelengths would call for long integration times that wouldn't be an efficient use of the ALMA science demonstration phase.

The high-*z* sample were all selected from the 4 Ms *Chandra* Deep Field South (hereafter, CDF-S) survey catalogue described in Xue et al. (2011) with updated redshifts from Hsu et al. (2014); for consistency, we recalculate the rest-frame 2-10 keV luminosities (L_X) of the sources using these new redshifts. To ensure reliable AGN selection, we only consider those sources with $L_X > 10^{42}$ ergs s^{-1} and reliable redshifts that lie within 6′ of the average aim point of the survey (the latter ensures highly reliable positions for matching to ALMA counterparts). As a primary science goal of this study is to constrain the (s)SFR distributions of moderate to high redshift AGN host galaxies in the context of the MS, we restrict our sample to AGNs with host galaxy stellar masses
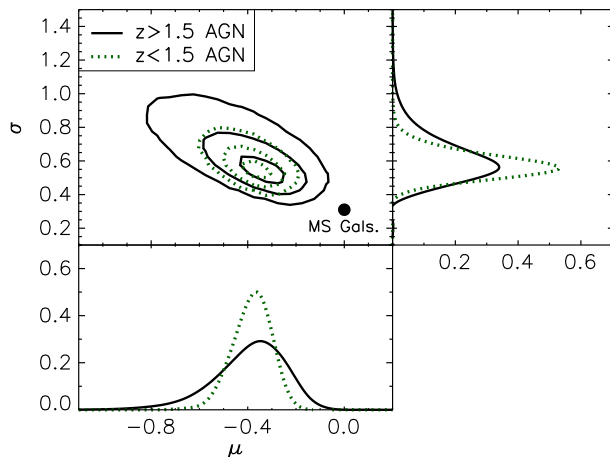
Figure 2. The posterior probability distributions (PDs) for the parameters describing the assumed log-normal R_{MS} distribution for AGN host galaxies: μ is the mode of the log-normal, while σ is its 1σ width (see Eq. 1). PDs for both our low-z and high-z samples are shown (see key). Contours of 20, 68 and 95 per cent confidence are shown. The best-fit parameters of the combined (i.e., redshift-averaged) R_{MS} distribution of MS galaxies is indicated by the solid black circle (from Schreiber et al. 2015). The bottom and rightmost plots indicate the relative probability of μ and σ values; the location of the peak represent the most probable parameter values. When modelled as a log-normal, the R_{MS} distribution of AGN host galaxies is significantly broader, and shifted significantly lower than that of MS galaxies.

(M_*; derived following Santini et al. 2012) above 2×10^{10} M$_\odot$ (all our AGN have rest-frame optical–near-IR colours and SEDs, from which M_* are derived, that are consistent with being host-dominated; see Mullaney et al. 2012a). Below this M_* threshold, it becomes prohibitive to reach low enough flux limits to probe to SFRs significantly below the mean SFR of MS galaxies (hereafter, SFR$_{MS}$) with ALMA. Despite this M_* cut we still sample a significant proportion of the luminous AGN population since the stellar mass distribution of galaxies hosting $L_X > 10^{42}$ ergs s^{-1} AGNs peaks at $\approx 6 \times 10^{10}$ M$_\odot$ (e.g., Fig. 14 of Mullaney et al. 2012a).

The above selection criteria returned 49 AGNs (our high-z sample). Of these, 13 are detected in the GOODS-*Herschel* 160 μm observations of the CDF-S (Elbaz et al. 2011) from which reliable SFRs can be derived. Of the remaining 36 AGNs, 24 were observed by ALMA. However, since making our original ALMA target list, a more sensitive *Herschel* 160 μm map of the CDF-S has been generated by combining the PEP (Lutz et al. 2011) and GOODS-*Herschel* surveys (Magnelli et al. 2013) and four of our 24 ALMA targets are now detected in that new map. For these four, we adopt the mean (s)SFR derived from the two facilities (see §3). All other *Herschel* fluxes and 3σ upper limits (including for the twelve *Herschel*-undetected AGNs not targeted by ALMA) are also taken from the combined PEP+GOODS-*Herschel* dataset.

The low-z sample were selected from the regions of the *Chandra* Deep Field North (from Alexander et al. 2003 and adopting the same redshifts and M_* as Mullaney et al. 2012a) and South (Xue et al. 2011, but using the updated redshifts and M_*) surveys with deep *Herschel* coverage by the combined PEP+GOODS surveys. We also restrict this low-z sample to $L_X > 10^{42}$ ergs s^{-1} and $M_* > 2 \times 10^{10}$ M$_\odot$ to allow meaningful comparison with the high-z sample. This returned a sample of 110 AGNs (i.e., our low-z sample), 65 (i.e., ~59 per cent) of which are detected in the *Herschel* 160 μm band, from which we derive (s)SFRs (see §3); 3σ flux upper limits were measured for the 45 *Herschel* non-detections.

Table 1. Best-fit parameters for the log-normal R_{MS} distributions (see Eqn. 1) of the samples of galaxies described in the main text.

(1) Sample	(2) μ	(3) σ
MS galaxies (Schreiber et al. 2015)	0	0.31 ± 0.02
Low-z AGN sample	$-0.378^{+0.068}_{-0.079}$	$0.568^{+0.082}_{-0.062}$
High-z AGN sample	$-0.38^{+0.12}_{-0.16}$	$0.59^{+0.15}_{-0.10}$
Combined AGN sample	$-0.369^{+0.065}_{-0.080}$	$0.560^{+0.087}_{-0.065}$

NOTES: Values given are the median of the posterior probability distributions (PDs) and the 68 per cent confidence intervals.

3   ALMA OBSERVATIONS AND DATA ANALYSIS

All 24 of our ALMA targets were observed with ALMA Band-7 (i.e., observed-frame ~ 850 μm) during November, 2013, with a longest baseline of 1.3 km. To maximise observing efficiency, the ALMA-targeted sample was split into three groups according to the flux limit required to probe down to at least SFR$_{MS}$ at a given redshift. This corresponds to RMS flux limits of 200 μJy, 125 μJy and 90 μJy for the three groups. ALMA continuum fluxes were measured using uv_fit of GILDAS v.apr14c, adopting point source profiles for two unresolved sources and circular Gaussian profiles for the other five detected targets.

Measured ALMA and *Herschel* fluxes and upper limits were converted to 8-1000 μm infrared luminosities (hereafter, L_{IR}) using our adopted redshifts (see §2) and the average infrared SEDs of MS galaxies described in Béthermin et al. (2015), which are constructed using the theoretical templates of Draine & Li (2007). However, we note that our main conclusions do not change if we instead use either the Chary & Elbaz (2001) SEDs or a starburst SED (i.e., Arp220). At the redshifts of our high-z sample, Band-7 probes the rest-frame 180–340 μm, close to the peak of the far-infrared emission due to star-formation. While these rest-frame wavelengths are also sensitive to dust mass (e.g., Scoville et al. 2014), based on the range of Draine & Li (2007) SED templates we estimate that the corresponding L_{IR} are accurate to within ± 0.3 dex, which we factor into our analyses. As a check, we note that the SFRs derived from ALMA and *Herschel* data for the four AGNs that are detected with both are consistent to within this tolerance. SFRs are derived from L_{IR} using Eqn. 4 from Kennicutt (1998), but adopting a Chabrier IMF. Finally, to explore the distributions of AGN host SFRs relative to SFR$_{MS}$, we define $R_{MS} \equiv$ SFR/SFR$_{MS}$, the relative offset from the MS, where SFR$_{MS}$ is computed using Eqn. 9 of Schreiber et al. (2015; hereafter, S15).

4   RESULTS

4.1   Star-forming properties of X-ray AGNs

The highly sensitive ALMA observations of $z > 1.5$ AGNs allow us to probe to SFRs that are up to a factor of ≈ 10 below that possible with *Herschel* (see Fig. 1). Despite this, only seven (i.e., ≈ 29 per cent) of the 24 ALMA-targeted AGNs in our high-z sample are detected at $> 3\sigma$ at 850 μm. However, by the design of our experiment, the 3σ upper limits provided by the ALMA+*Herschel* data enable us to infer the level of consistency between the distributions of R_{MS} for AGN and MS galaxies (see §4.2), the latter of which has been shown not to vary in the M_* and redshifts ranges considered here (e.g., Rodighiero et al. 2011; Sargent et al. 2012, S15).

First, however, we consider the host galaxy SFRs of the AGNs in our two samples as a function of redshift, shown in Fig. 1, upper panel. A striking feature of this plot is that the majority (i.e., 142/159≈89 per cent) of all AGNs in our samples reside in sub-ULIRG (i.e., $< 10^{12}$ L$_\odot$) galaxies. Furthermore, we find no evidence that the more luminous AGNs (i.e., quasars with $L_X > 10^{44}$ ergs s^{-1}) in our sample preferentially reside in the most strongly star-forming systems, although we acknowledge the small number of quasars in our sample may obscure such trends with luminosity (e.g., Harrison et al. 2012).

To explore our AGN hosts' star-forming properties in the context of the evolving MS, we plot their sSFRs and R_{MS} values as a function of redshift (Fig. 1, middle and lower panels, respectively). We find that 54 to 88 (range due to upper limits) of the 159 AGNs (i.e., ≈34 to ≈55 per cent) in our combined (i.e., low-z+high-z) sample have $R_{MS} < 0.5$, with significant overlap between the fractions in our low-z (i.e., ≈43 per cent to ≈54 per cent) and high-z (i.e., ≈14 per cent to ≈59 per cent) samples. Comparing these fractions to the ≈15 per cent of MS galaxies with $R_{MS} < 0.5$ (from S15), reveals that the AGNs in our low-z sample, and possibly also our high-z sample, do not trace the same R_{MS} distribution as MS galaxies, instead displaying a strong bias toward lower R_{MS} values. Finally, we note that only ≈5 per cent of AGNs in our combined sample reside in starbursts (i.e., with $R_{MS} > 4$).

4.2   Parameterising an X-ray AGN SFR distribution

In the previous subsection we reported that the large fraction of AGNs with $R_{MS} < 0.5$ in our combined and, in particular, low-z samples is inconsistent with the R_{MS} distribution of MS galaxies. In this subsection, we attempt to place constraints on the distribution of SFRs (relative to the MS; i.e., R_{MS}) of AGN hosts, taking both detections and upper limits into account. We place particular emphasis on quantifying the level of consistency/discrepancy between the AGN and MS R_{MS} distributions.

Unfortunately, our relatively small sample sizes, combined with the large fraction of non-detections prevents us from determining the R_{MS} distribution of AGN hosts directly. Since a key goal here is to quantitatively compare the AGN and MS R_{MS} distributions, we instead *assume* the same log-normal form for the AGN R_{MS} distribution as found for MS galaxies (e.g., Rodighiero et al. 2011; Sargent et al. 2012, S15):

$$N(R_{MS}) \propto \exp\left(-\frac{(\log(R_{MS}) - \mu)^2}{2\sigma^2}\right) \qquad (1)$$

and infer its parameters (i.e., similar to Shao et al. 2010 who inferred the AGN L_{IR} distribution). This is done purely to ease comparison between the AGN and MS R_{MS} distributions by allowing us to compare like-for-like parameters (i.e., the mode, μ, and the variance, σ^2, of the adopted log-normal R_{MS} distribution), and is not to be taken as a literal description of the true AGN R_{MS} distribution.[1]

We adopt a hierarchical Bayesian framework to determine the best-fit parameters (i.e., μ and σ) for our assumed log-normal distributions, using Gibbs sampling and the Metropolis-Hastings MCMC algorithm to randomly sample their posterior probability distributions (hereafter, PDs; Gelman et al. 2014). The benefits of taking this approach are that (a) upper limits and uncertainties on

[1] Investigating whether other forms better describe the R_{MS} distribution of AGN hosts will be the focus of a later study incorporating a larger set of ALMA observations from Cycle 2 (PI: Alexander; awaiting completion).
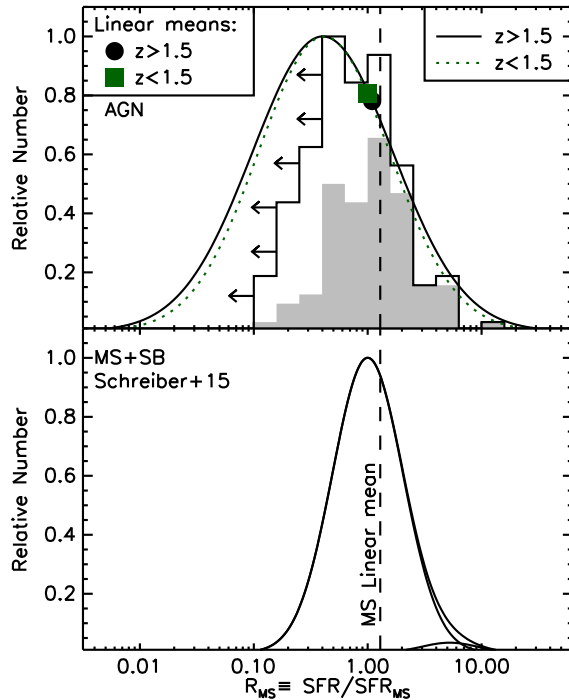
Figure 3. R_{MS} distributions for our high-z and low-z samples of X-ray selected AGNs (*Top*) and MS galaxies (*Bottom*). Here, we show the log-normal distributions with best fitting parameters shown in Table 1 (solid and dotted curves; see key). The histograms in the top panel shows the relative numbers of AGNs from our combined (i.e., low-z+high-z) sample in each R_{MS} bin; the solid grey histogram represents those AGNs detected at $> 3\sigma$ with either *Herschel* or ALMA, whereas the empty histogram (with left-pointing arrows) also includes upper limits. The solid points in the top panel indicate the linear means of the log-normal distributions (equivalent to what would be obtained via, e.g., stacking analyses) and lie within 1σ of the linear mean R_{MS} of MS galaxies (vertical dashed line).

R_{MS} can be readily taken into account and (b) the resulting posterior PDs provide us with meaningful parameter uncertainties. We use weak prior PDs, noting that the centring of these priors (within reasonable limits) has no significant effect on our results.

The posterior PDs on μ and σ for our two samples are presented in Fig. 2, while the best-fit parameters (median of the PDs and 68 per cent confidence intervals) are given in Table 1. For comparison, we also include the best-fit parameters of the log-normal R_{MS} distribution for non-AGN MS galaxies from S15. As expected from the smaller size of our AGN sample and the high fractions of non-detections compared to the MS galaxy sample of S15, the uncertainties on the posterior parameter values for the assumed AGN log-normal R_{MS} distribution are considerably larger than those for MS galaxies. Despite this, our analysis shows that the R_{MS} distributions of our low-z and high-z AGNs are both significantly broader and peak at significantly lower values (both at > 99.9 per cent confidence) than that of MS galaxies. Interestingly, our analyses show that, as with MS galaxies, there appears to be little evolution in the AGN R_{MS} distribution, with the modes and variances of the log-normal distributions describing our low-z and high-z samples being consistent to within 1σ. In light of this, we infer the R_{MS} distribution of our combined sample, which we find is roughly twice as broad as, and peaks ≈0.4 dex below, that of MS galaxies (Table 1).

5   INTERPRETATION

In the previous section we used our combined ALMA+*Herschel* data to demonstrate that the R_{MS} distributions of X-ray selected AGNs differ significantly from that of MS galaxies. Indeed, when modelled as a log-normal, the AGN R_{MS} distribution is significantly broader and peaks at significantly lower values than that of MS galaxies. This result appears to be at-odds with recent findings, based on mean-stacked *Herschel* data, that the average star-forming properties of AGN hosts is broadly consistent with those of MS galaxies (e.g., Mullaney et al. 2012a; Santini et al. 2012; Rosario et al. 2013). In this section, we place our results in the context of these studies to explore the root of these apparent discrepancies.

When comparing to the results derived from mean-stacked *Herschel* data, it is important to note that stacking provides a linear mean which does not correspond to the mode, μ, of a log-normal distribution. Instead, the linear mean will *always* be higher than the mode. Furthermore, the discrepancy between the linear mean and the mode increases strongly as function of both μ and σ.

We can compare our results against those from stacking by calculating the linear mean of our log-normal distributions, taking a Monte-Carlo approach to sample the μ and σ PDs. This gives linear-mean AGN R_{MS} values (i.e., $\langle R_{MS} \rangle$) of $0.99^{+0.23}_{-0.16}$ and $1.09^{+0.47}_{-0.25}$ for our low-z and high-z samples, respectively (Fig. 3). These values (and thus, by extension, our derived distributions) are remarkably consistent with the linear means derived from mean-stacked *Herschel* data (i.e., $\langle R_{MS} \rangle \approx 1$; e.g, Mullaney et al. 2012a). We therefore conclude that these means are, indeed, strongly influenced by the high tail of the broad R_{MS} distribution and thus may not necessarily give a reliable indication of the modal SFR of AGN hosts.

Despite finding that the R_{MS} distribution of AGN hosts is shifted toward lower values compared to MS galaxies, our results remain consistent with AGNs preferentially residing in galaxies with comparatively high (s)SFRs by $z \sim 0$ standards due to the strong redshift evolution of SFR_{MS}. Indeed, applying our analyses to sSFR (rather than R_{MS}) gives distributions peaking at ≈ 0.2 Gyr^{-1} and ≈ 0.5 Gyr^{-1} for our low-z and high-z samples, respectively. To put this in context, $\langle sSFR_{MS} \rangle \approx 0.1$ Gyr^{-1} at $z \approx 0$, thus local galaxies with sSFRs of 0.2 Gyr^{-1} and 0.5 Gyr^{-1} would be classed as MS and starbursting galaxies, respectively.

The results presented here compare favourably to those derived from AGN surveys conducted at other wavelengths. For example, using SFRs derived from optical SED fitting, Bongiorno et al. (2012) reported a broad sSFR distribution for X-ray selected AGNs that peaks at values below that of the MS at redshifts similar to those explored here (i.e., $0.3 < z < 2.5$). Similarly, Azadi et al. (2014) showed that the R_{MS} (referred to as the "epoch-normalised" sSFR in their paper) distribution of X-ray selected AGNs (with a similar M_* selection as here) peaks at ~ 0.1 and is similar (if shifted to slightly higher values) to the R_{MS} distribution of M_*-matched galaxies (i.e., not just star-forming galaxies). As such, these studies and the results presented here support the view that X-ray selected AGN hosts at moderate to high redshifts span the full range of *relative* sSFRs of $M_* \gtrsim 2 \times 10^{10}$ M$_\odot$ galaxies (e.g., Georgakakis et al. 2014), but tend to be star-forming by $z \sim 0$ standards.

REFERENCES

Aird, J., Coil, A. L., Georgakakis, A., et al. 2015, ArXiv e-prints, 1503.01120

Alexander, D. M., & Hickox, R. C. 2012, New Astron. Rev., 56, 93

Alexander, D. M., Bauer, F. E., Brandt, W. N., et al. 2003, AJ, 126, 539

Azadi, M., Aird, J., Coil, A., et al. 2014, ArXiv e-prints, 1407.1975

Béthermin, M., Daddi, E., Magdis, G., et al. 2015, A&A, 573, A113

Bongiorno, A., Merloni, A., Brusa, M., et al. 2012, MNRAS, 427, 3103

Chary, R., & Elbaz, D. 2001, ApJ, 556, 562

Chen, C.-T. J., Hickox, R. C., Alberts, S., et al. 2013, ApJ, 773, 3

Daddi, E., Dickinson, M., Morrison, G., et al. 2007, ApJ, 670, 156

Delvecchio, I., Lutz, D., Berta, S., et al. 2015, ArXiv e-prints, 1501.07602

Draine, B. T., & Li, A. 2007, ApJ, 657, 810

Elbaz, D., Dickinson, M., Hwang, H. S., et al. 2011, A&A, 533, A119

Gebhardt, K., Bender, R., Bower, G., et al. 2000, ApJL, 539, L13

Gelman, A., Carlin, J. B., Stern, H. S., et al. 2014, Bayesian Data Analysis, 3rd. ed

Georgakakis, A., Pérez-González, P. G., Fanidakis, N., et al. 2014, MNRAS, 440, 339

Harrison, C. M., Alexander, D. M., Mullaney, J. R., et al. 2012, ApJL, 760, L15

Hsu, L.-T., Salvato, M., Nandra, K., et al. 2014, ApJ, 796, 60

Kennicutt, Jr., R. C. 1998, ARA&A, 36, 189

Lutz, D., Poglitsch, A., Altieri, B., et al. 2011, A&A, 532, A90

Magnelli, B., Popesso, P., Berta, S., et al. 2013, A&A, 553, A132

Mullaney, J. R., Pannella, M., Daddi, E., et al. 2012a, MNRAS, 419, 95

Mullaney, J. R., Daddi, E., Béthermin, M., et al. 2012b, ApJL, 753, L30

Noeske, K. G., Weiner, B. J., Faber, S. M., et al. 2007, ApJL, 660, L43

Rodighiero, G., Daddi, E., Baronchelli, I., et al. 2011, ApJL, 739, L40

Rodighiero, G., Brusa, M., Daddi, E., et al. 2015, ApJL, 800, L10

Rosario, D. J., Trakhtenbrot, B., Lutz, D., et al. 2013, A&A, 560, A72

Rosario, D. J., McIntosh, D. H., van der Wel, A., et al. 2015, A&A, 573, A85

Santini, P., Rosario, D. J., Shao, L., et al. 2012, A&A, 540, A109

Sargent, M. T., Béthermin, M., Daddi, E., & Elbaz, D. 2012, ApJL, 747, L31

Schaye, J., Crain, R. A., Bower, R. G., et al. 2015, MNRAS, 446, 521

Schreiber, C., Pannella, M., Elbaz, D., et al. 2015, A&A, 575, A74

Scoville, N., Aussel, H., Sheth, K., et al. 2014, ApJ, 783, 84

Shao, L., Lutz, D., Nordon, R., et al. 2010, A&A, 518, L26

Silverman, J. D., Green, P. J., Barkhouse, W. A., et al. 2008, ApJ, 679, 118

Stanley, F., Harrison, C. M., Alexander, D. M., et al. 2015, ArXiv e-prints, 1502.07756

Vogelsberger, M., Genel, S., Springel, V., et al. 2014, MNRAS, 444, 1518

Xue, Y. Q., Luo, B., Brandt, W. N., et al. 2011, ApJS, 195, 10